

Stable mononuclear rhodium(II) polypyridyl complexes: synthesis, spectroscopic and structural characterisation

Parimal Paul,* Beena Tyagi, Anvarhusen K. Bilakhiya, Mohan M. Bhadbhade and E. Suresh

Discipline of Silicates and Catalysis, Central Salt and Marine Chemicals Research Institute, Bhavnagar 364 002, India. E-mail: salt@cscsmcri.ren.nic.in

Received 28th January 1999, Accepted 13th March 1999

The reaction of $\text{RhCl}_3 \cdot 3\text{H}_2\text{O}$ and 2,4,6-tris(2-pyridyl)-1,3,5-triazine (tptz) in refluxing ethanol–water (1 : 1) resulted in the hydrolysis of tptz to bis(2-pyridylcarbonyl)amide anion (bpca) and afforded a mixture of Rh^{III} and Rh^{II} complexes which were separated and characterised as $[\text{Rh}^{\text{III}}(\text{bpca})_2][\text{PF}_6]$ and $[\text{Rh}^{\text{II}}(\text{bpca})_2] \cdot 3\text{H}_2\text{O}$ **1**. Similarly the reaction of tptz and $\text{Rh}(\text{tpy})\text{Cl}_3$ (tpy = 2,2' : 6',2''-terpyridyl) yielded mixed ligand complexes $[\text{Rh}^{\text{III}}(\text{bpca})(\text{tpy})]^{2+}$ and $[\text{Rh}^{\text{II}}(\text{bpca})(\text{tpy})]\text{Cl} \cdot 8\text{H}_2\text{O}$ **2**. The molecular structures of complexes **1** and **2** have been established by single-crystal X-ray analysis. In complex **1** two bpca moieties are co-ordinated to Rh^{II} with nitrogen as donor atoms in a mutually perpendicular fashion. In complex **2** bpca and tpy are bound to the metal ion in a similar fashion to that found in **1**. The axial Rh–N bond distances in **1** and **2** are significantly shorter compared to equatorial Rh–N bond distances, indicating an axially compressed octahedral geometry of the metal ion. Complexes **1** and **2** exhibit absorption bands in the 545–600 nm region whereas their Rh^{III} analogues do not show any band in this region. Electrochemical studies of **1** and **2** revealed a metal based reduction ($\text{Rh}^{\text{III}} \rightarrow \text{Rh}^{\text{II}}$) at -1.13 and -0.72 V, respectively, followed by two ligand-based redox couples. EPR studies of **1** and **2** in acetonitrile at 77 K show $g_{\parallel} > g_{\perp} \approx g_e$ indicating a $d_{x^2-y^2}$ ground state and a compressed octahedral geometry for the metal ion, consistent with the crystal structures.

Introduction

The co-ordination chemistry of rhodium is dominated by its +1 and +3 oxidation states. Among known $\text{Rh}(\text{II})$ complexes diamagnetic dimers with an Rh–Rh bond are the most common.^{1–5} Only a limited number of reports have addressed mononuclear paramagnetic $\text{Rh}(\text{II})$ complexes.^{6,7} The stability of the mononuclear complexes depends mainly on the structural and electronic properties of the ligands. Many of those complexes were stabilised using sterically crowded ligands such as tertiary phosphine, porphyrins, crown thioethers, Schiff bases, arynes and hydrotris(pyrazolyl) borate.^{6–8} Molecular geometries of only a few of these complexes have been established by single-crystal X-ray studies.^{8–16} However, using poly(pyridyl) ligands a few dimeric $\text{Rh}(\text{II})$ complexes have been isolated^{5,17} but no stable monomer has been reported with the exception $[\text{Rh}(\text{bipy})_2][\text{NO}_3]$.¹⁸ However, short-lived Rh^{II} mononuclear complexes were generated by one-electron reduction of the corresponding Rh^{III} complexes either photochemically^{19–21} or electrochemically^{22,23} and their properties were studied in solution. Generally, when mononuclear octahedral Rh^{III} complexes are reduced to Rh^{II} they undergo ligand labilization, which results in the loss of one ligand and either dimerization or disproportionation to Rh^{III} and Rh^{I} species.^{19–23}

Recently we studied the reaction of RhCl_3 with 2,4,6-tris(2-pyridyl)-1,3,5-triazine (tptz), which in ethanol–water resulted in the hydrolysis of tptz to the bis(2-pyridylcarbonyl)amide anion (bpca) and afforded a mixture of Rh^{III} and Rh^{II} complexes, the Rh^{III} complex was characterised as $[\text{Rh}^{\text{III}}(\text{bpca})_2][\text{PF}_6]$.²⁴ The reaction of $\text{Rh}(\text{tpy})\text{Cl}_3$ (tpy = 2,2' : 6',2''-terpyridine) with tptz also promoted the hydrolysis of tptz to bpca and yielded a mixture of mixed ligand complexes of Rh^{III} and Rh^{II} . The Rh^{III} complex, $[\text{Rh}(\text{bpca})(\text{tpy})][\text{PF}_6]$ has also been reported.²⁵ The Rh^{II} complexes (minor products) were separated successfully from their Rh^{III} analogues. Herein, we report the synthesis, purification, spectroscopic and structural characterisation of these two rare examples of mononuclear Rh^{II} complexes.

Experimental

Materials

Sephadex SP C-25 and the ligand 2,2' : 6',2''-terpyridine and tetrabutylammonium tetrafluoroborate were obtained from Aldrich. Hydrated rhodium trichloride was obtained from Arora Matthey. Solvents were purified by standard methods before use.

Physical measurements

Elemental analyses (C, H, N) were performed on a model 2400 Perkin-Elmer Elemental Analyser. UV/VIS spectra were recorded on a model 8452A Hewlett-Packard Diode Array spectrophotometer. EPR studies were performed on a Bruker ESP 300 X-band spectrometer attached to an ESP 1600 data system. Electrochemical measurements were carried out with a model 273A EG & G Princeton Applied Research Potentiostat. All electrochemical experiments were conducted in an argon atmosphere with a glassy carbon working electrode. A saturated calomel electrode (SCE) was used as reference with 0.1 mol dm^{-3} $[\text{NBu}_4][\text{BF}_4]$ as the supporting electrolyte.

Syntheses

$[\text{Rh}(\text{bpca})_2] \cdot 3\text{H}_2\text{O}$ **1.** A mixture of tptz (624 mg, 2 mmol) and $\text{RhCl}_3 \cdot 3\text{H}_2\text{O}$ (264 mg, 1 mmol) in ethanol–water (1 : 1, 60 cm^3) was refluxed under an argon atmosphere for 45 h. The volume of the reaction mixture was reduced to ca. 20 cm^3 by rotary evaporation and an aqueous solution (5 cm^3) of NH_4PF_6 (326 mg, 2 mmol) was added. The resulting precipitate ($[\text{Rh}^{\text{III}}(\text{bpca})_2][\text{PF}_6]$) was filtered off and washed with water (5 cm^3 , three times). The filtrate and washing were collected and evaporated to dryness by rotary evaporation. The crude solid was chromatographed on deactivated alumina (5% H_2O) in acetonitrile–water (9 : 1). After removal of a minor first fraction the desired compound was separated as a greenish brown solution which was kept at room temperature allowing slow evaporation. After ten days a crystalline compound suitable for single

Table 1 Summary of crystallographic data and parameters for complexes **1** and **2**

	1	2
Empirical Formula	C ₂₄ H _{23.6} N ₆ O _{7.8} Rh	C ₂₇ H ₃₅ N ₆ O ₁₀ ClRh
<i>M</i>	623.80	741.97
Crystal system	Monoclinic	Triclinic
Space group	<i>C2/c</i>	<i>P</i> $\bar{1}$
Crystal dimensions/mm	0.14 × 0.10 × 0.08	0.22 × 0.09 × 0.05
<i>a</i> /Å	23.410(4)	9.072(4)
<i>b</i> /Å	16.013(7)	11.749(3)
<i>c</i> /Å	15.006(8)	16.605(5)
<i>a</i> °		75.09(2)
<i>β</i> °	108.23(3)	77.14(3)
<i>γ</i> °		89.52(3)
<i>U</i> /Å ³	5343.0(4)	1665.1(10)
<i>Z</i>	8	2
<i>D</i> /g cm ⁻³	1.551	1.480
<i>F</i> (000)	2536	762
<i>μ</i> (Mo-K α)/mm ⁻¹	0.697	0.654
Total reflections	4679	5843
Observed reflections [<i>I</i> > 2 σ (<i>I</i>)]	3686	5292
Parameters refined	360	406
Final <i>R1</i> (on <i>F</i>) ^a	0.059	0.044
Final <i>wR2</i> (on <i>F</i> ²) ^b	0.187	0.141

^a $R1 = \sum ||F_o| - |F_c|| / \sum |F_o|$. ^b $wR2 = [\sum w(F_o^2 - F_c^2)^2] / \sum [w(F_o^2)^2]^{1/2}$.

crystal X-ray study was obtained. Yield: 20% (Found: C, 47.04; H, 3.81; N, 13.52. Calc. for C₂₄H₂₂N₆O₇Rh: C, 47.30; H, 3.64; N, 13.79%). Molar conductance ($A_M/\Omega^{-1} \text{ cm}^2 \text{ mol}^{-1}$): 16 (non-electrolyte). $\lambda_{\text{max}}/\text{nm}$ ($\epsilon/\text{dm}^3 \text{ mol}^{-1} \text{ cm}^{-1}$) (acetonitrile): 270 (20400), 335sh (4700), 400sh (1300), 545sh (235) and 592 (310).

[Rh(bpca)(tpy)]Cl·8H₂O 2. [Rh(tpy)Cl₃]²⁵ (442 mg, 1 mmol) and tptz (312 mg, 1 mmol) were refluxed in ethanol–water (1 : 1, 60 cm³) under an argon atmosphere for 40 h. The solution was then concentrated to ca. 20 cm³ and chromatographed on a Sephadex SP C-25 column with an aqueous 0.05 mol dm⁻³ solution of sodium chloride as eluent. After separation of a small first fraction complex **2** was separated and finally the Rh^{III} complex was eluted using a 0.2 mol dm⁻³ solution of sodium chloride. Solvent was removed from the desired fraction in a rotary evaporator and the residue was extracted with dry ethanol (5 cm³), the process was repeated three times, the solid mass was then dissolved in acetonitrile–water (1 : 1, 10 cm³) and allowed slowly to evaporate at room temperature. After 15 days a crystalline compound suitable for X-ray study was separated. Yield: 14% (Found: C, 43.46; H, 4.92; N, 11.08. Calc. for C₂₇H₃₅N₆O₁₀ClRh: C, 43.71; H, 4.75; N, 11.33%). Molar conductance ($A_M/\Omega^{-1} \text{ cm}^2 \text{ mol}^{-1}$): 148 (1 : 1 electrolyte). $\lambda_{\text{max}}/\text{nm}$ ($\epsilon/\text{dm}^3 \text{ mol}^{-1} \text{ cm}^{-1}$) (acetonitrile): 280 (22800), 326 (11800), 338 (10500), 356 (7000), 410sh (550), 552 (375) and 600 (170).

Crystal structure determination

Preliminary data on the space group and unit cell dimensions as well as intensity data were collected on an Enraf-Nonius CAD4 X-ray diffractometer using graphite-monochromatised Mo-K α radiation ($\lambda = 0.7107 \text{ \AA}$) in the range θ 2–23°. Accurate cell dimensions were obtained using 25 high angle reflections ($10 < \theta < 14$). The crystal orientation, refinement of cell parameters and intensity measurements were carried out using the program CAD-4 PC.²⁶ Intensities were corrected for Lorentz-polarisation effects but not for absorption. The Lorentz-polarisation correction and data reduction were carried out using the NRCVAX program.²⁷ The structure was solved by the heavy-atom method using the program SHELXL 97.²⁸ Intermolecular calculations were carried out using the program CSU.²⁹ All computations were performed on a Pentium-Pro PC. Crystallographic data for complexes **1** and **2** are summarised in Table 1.

For complex **1**, the difference Fourier map after the anisotropic refinement of non-hydrogen atoms of [Rh(bpca)₂] contained one peak of height 9.2 e Å⁻³ and eleven other peaks of height varying from 4.9 to 1.19 e Å⁻³. These peaks were assigned to water molecules, the first one with full occupancy and others with partial occupancies according to peak height. The occupancies of oxygen atoms were refined using SHELXL 97.

For complex **2**, after the anisotropic refinement of non-hydrogen atoms of [Rh(bpca)(tpy)]Cl the difference map revealed seven peaks of height 7.6 to 6 e Å⁻³ followed by two peaks of height 3.5 and 3.3 e Å⁻³. As in complex **1**, the first seven peaks were assigned to seven water molecules with full occupancies and refined anisotropically and the last two were assigned to a two component disordered water molecule and refined by using the FVAR facility in SHELXL 97. The H-atoms of the bpca and tpy moieties were fixed stereochemically and refined using a riding model. The H-atoms of the water molecules with full occupancies were modelled taking into account their H-bonding interactions using the program CSU.²⁹

CCDC reference number 186/1424.

See <http://www.rsc.org/suppdata/dt/1999/2009/> for crystallographic files in .cif format.

Results and discussion

Synthesis of the complexes

The reaction of rhodium trichloride and tptz in refluxing ethanol–water resulted in the hydrolysis of tptz to the bis(2-pyridylcarbonyl)amide anion (bpca) and afforded Rh^{III} and Rh^{II} complexes of composition [Rh(bpca)₂]^{*n*+} (*n* = 0 and 1). Similarly, the reaction of [Rh(tpy)Cl₃] and tptz yielded complexes of composition [Rh(bpca)(tpy)]^{*n*+} (*n* = 1 and 2). In both cases the Rh^{II} complexes were the minor products. The addition of NH₄PF₆ to the [Rh(bpca)₂]^{*n*+} mixture allowed the isolation of Rh^{III} complex as its PF₆⁻ salt, [Rh(bpca)₂][PF₆]. The Rh^{II} complex is a neutral species (*n* = 0) and it remained in solution from which it was isolated and purified by column chromatography on deactivated alumina.

In the [Rh(bpca)(tpy)]^{*n*+} mixture both the complexes are cations and the separation was carried out by ion-exchange chromatography on Sephadex. From the eluent the desired complex can be isolated as its PF₆⁻ anion but the Cl⁻ salt gave better quality crystals for X-ray study. The Rh^{III} complexes were pale yellow and those of Rh^{II} were greenish brown. The ligand (tptz) and complexes **1** and **2** are shown in Scheme 1.

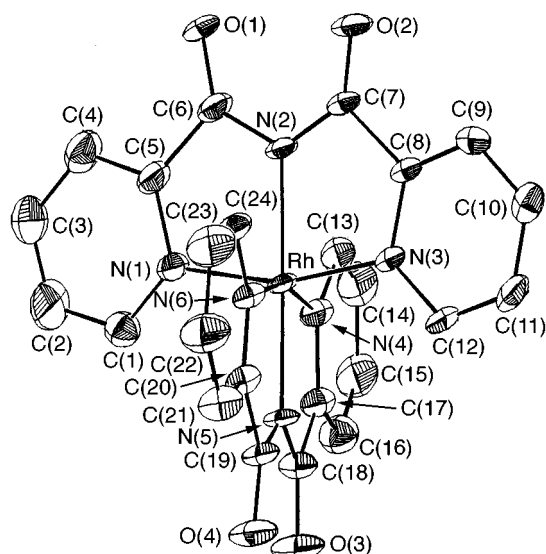
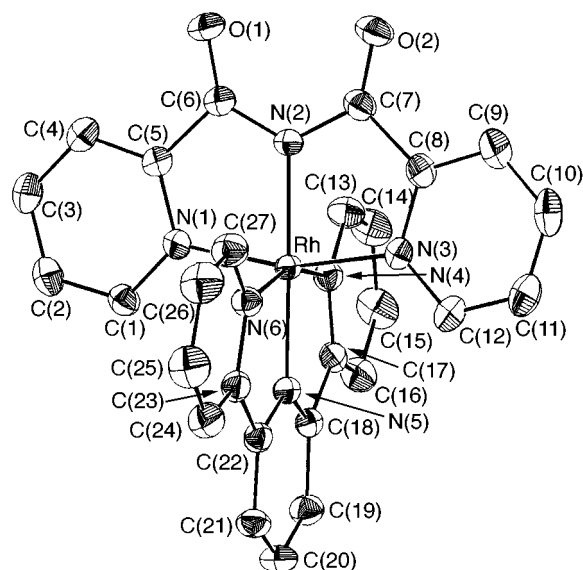
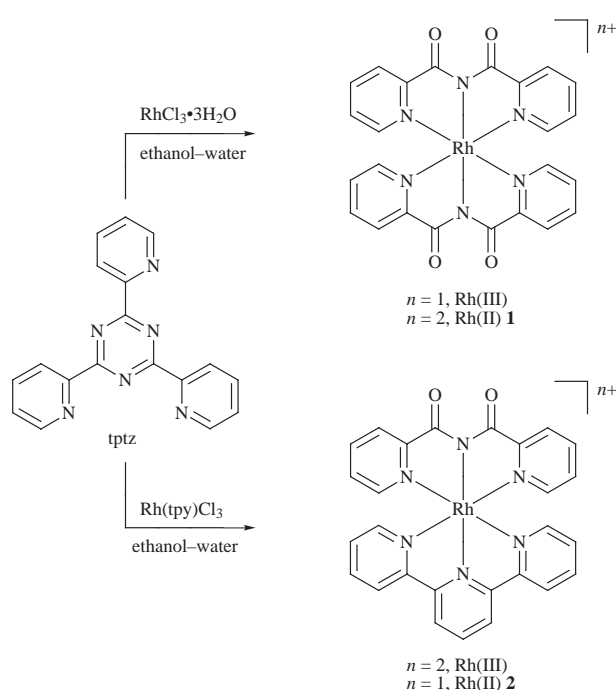
The reduction of Rh^{III} to Rh^{II}, induced by ligand or solvent has been known for many years. It is common in the reactions between hydrated rhodium(III) chloride and phosphines in ethanol⁷ but is also found in the presence of other ligands such as lithium aryl (2,4,6-triisopropylphenyl), C₆Me₆, 5,5'-thiodisallylic acid and NO.^{7,13} It has also been reported that the reaction between rhodium trichloride hydrate and bulky phosphine resulted in a mixture of rhodium(III) and rhodium(II) complexes.^{12,30} Our observations, therefore, are similar to some earlier reports with different types of ligands.^{12,30}

Crystal structures

ORTEP³¹ views of complexes **1** and **2** along with their atom numbering schemes are shown in Figs. 1 and 2, respectively. Selected bond distances and angles of both the complexes are presented in Table 2. The tridentate bpca ligands in **1** and tridentate bpca and tpy in **2** are bound to the metal ion almost in a mutually perpendicular fashion forming a distorted octahedral geometry around the rhodium(II) centre. In both complexes **1** and **2** the middle nitrogen atoms [N(2) and N(5)] of the ligands are at the axial positions and the nitrogen atoms of the wing pyridyl rings [N(1), N(3), N(4) and N(6)] formed the equatorial

Table 2 Selected bond distances (Å) and angles (°) for complexes **1** and **2**

	1	2		1	2
Rh–N(1)	2.059(5)	2.024(3)	Rh–N(6)	2.022(5)	2.046(3)
Rh–N(2)	1.990(5)	1.990(3)	C(6)–O(1)	1.198(7)	1.202(6)
Rh–N(3)	2.036(5)	2.023(3)	C(7)–O(2)	1.165(7)	1.205(6)
Rh–N(4)	2.043(5)	2.049(4)	C(18)–O(3)	1.207(7)	—
Rh–N(5)	1.997(5)	1.963(3)	C(19)–O(4)	1.219(7)	—
N(1)–Rh–N(4)	93.18(19)	92.80(14)	N(2)–Rh–N(5)	178.5(2)	179.33(13)
N(1)–Rh–N(6)	89.55(19)	89.47(14)	N(2)–C(6)–C(5)	111.6(2)	110.9(4)
N(3)–Rh–N(4)	91.0(2)	90.65(14)	N(2)–C(7)–C(8)	110.9(5)	111.0(4)
N(3)–Rh–N(6)	91.4(2)	92.66(14)	N(5)–C(18)–C(17)	111.9(5)	112.8(3)
N(1)–Rh–N(3)	163.22(17)	163.22(14)	N(5)–C(19)–C(20)	111.8(5)	—
N(4)–Rh–N(6)	162.38(18)	160.76(14)	N(5)–C(22)–C(23)	—	112.9(4)

**Fig. 1** An ORTEP (50% probability) view of complex **1** with the atom labelling scheme shown; water molecules and hydrogen atoms are omitted for clarity.**Fig. 2** An ORTEP (50% probability) view of the cation of complex **2** with the atom labelling scheme; hydrogen atoms are omitted for clarity.

base. The *trans* angles of the axial nitrogens [N(2)–Rh–N(5) 178.5(2) in **1** and 179.33(13)° in **2**] are very close to the ideal value of 180°. The same angles for the equatorial nitrogens

deviate significantly [160.76(14)–163.22(17)°] from the ideal value indicating a tetrahedral distortion in the equatorial base, which may be due to constraints imposed by the five-membered chelate ring. The axial Rh–N distances in both complex **1** and **2** are significantly shorter compared to the equatorial Rh–N distances (Table 2) indicating an axially compressed octahedral geometry of the rhodium ion. The wing pyridyl rings of the bpa and tpy ligands in both complexes show slight deviations from their mean plane.

In complex **1** the amido oxygen atoms of both bpa moieties make strong intermolecular C–H···O interactions³² essentially along the *ab*-plane, forming a polymeric network as illustrated in Fig. 3. It is interesting to note that the C–H···O interaction from both the bpa moieties is different, O(1) and O(2) make a bifurcated H-bond with the pyridyl carbon C(12); whereas O(3) and O(4) each make a single interaction with C(1) and C(24), respectively (Table 3). The disordered water molecules are distributed within the cavity created by the molecule along the *ab*-plane.

In complex **2** the molecular cations in the unit cell can be described as H-bonded dimers *via* bifurcated C–H···O interactions³² between the oxygen atoms of the bpa moiety [O(1) and O(2)] and the C(13) of the tpy as illustrated in Fig. 4(a). The Cl[−] also shows a short C–H···Cl contact with C(24) of tpy. The water molecules are distributed around the dimers as shown in Fig. 4(b) and show strong H-bonding among themselves.

Electronic spectra

The electronic spectra of complexes **1** and **2** were recorded in

Table 3 Hydrogen bonding parameters (excluding water molecules) in complexes **1** and **2**

Complex	D ^a	H ^b	A ^c	D...A/Å	H...A/Å	D-H...A/°	Symmetry code
1	C(12)	H(12)	O(1)	3.152(1)	2.55(7)	122(5)	$x, 1 - y, -1/2 + z$
	C(12)	H(12)	O(2)	2.958(1)	2.165(8)	144(6)	$x, 1 - y, -1/2 + z$
	C(1)	H(1)	O(3)	3.06(8)	2.483(4)	121(1)	$1/2 - x, 1/2 - y, -z$
	C(24)	H(24)	O(4)	3.205(5)	2.542(2)	128(3)	$x, 1 - y, 1/2 + z$
2	C(13)	H(13)	O(1)	3.154(1)	2.49(2)	128(3)	$1 - x, 1 - y, -z$
	C(13)	H(13)	O(2)	3.066(3)	2.32(1)	136(3)	$1 - x, 1 - y, -z$
	C(24)	H(24)	Cl	3.678(3)	2.79(3)	159(3)	$x, 1 - y, 1/2 + z$

^a D = Donor. ^b H = Hydrogen. ^c A = Acceptor.

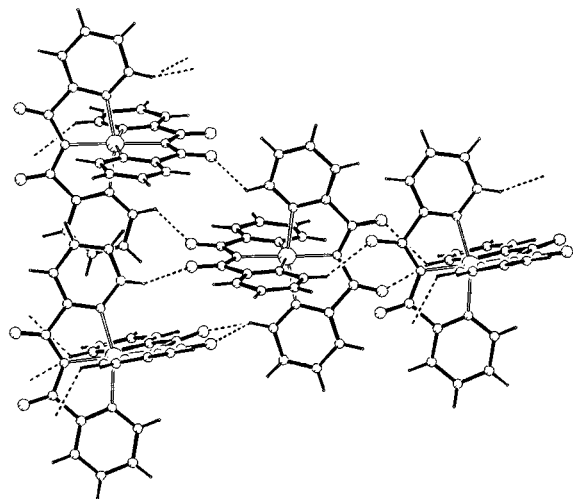


Fig. 3 A view showing the C-H...O interactions involving amido oxygen atoms of the bpca moieties of complex **1**.

acetonitrile. The spectra of complex **1** and its Rh^{III} analogue are illustrated in Fig. 5. In the visible region complex **1** exhibits a band at 592 nm and a shoulder at 545 nm, complex **2** also shows absorption maxima at 600 and 552 nm whereas their Rh^{III} analogues did not show any band above the 400 nm region (Fig. 5). In the low-spin Rh(II) (d⁷) mononuclear complexes a close similarity was noted between the electronic spectra of six-coordinate, five-coordinate square pyramidal and four-coordinate square-planar complexes.⁶ Most of these complexes exhibit two or more absorption bands in the 530–600 nm region,^{6,30,33,34} similar to that found in complexes **1** and **2** and those bands can be assigned to d–d transitions.^{6,10} The bands in the UV region of complexes **1** and **2** are similar to those of their Rh^{III} analogues except for a small shift of the absorption maxima around 270 nm and a significant decrease in the ϵ value of the band at \approx 330 nm in complex **1**.

Electrochemistry

The cyclic voltammograms of complexes **1** and **2** were recorded in acetonitrile. Complex **1** shows reductions at -1.13 (ΔE 70), -1.44 (122 mV) and -1.84 V vs. SCE, the reduction waves of complex **2** appear at -0.72 , -1.48 (ΔE 94 mV) and -1.80 V. In both complexes the last peak is poorly resolved in the cyclic voltammograms but well resolved in the square wave. The peak potentials of the complexes are similar to those of their Rh^{III} analogues but the cathodic current for the first reduction peak of the Rh^{II} complexes is almost half that of their Rh^{III} analogues (I_c Rh^{II}/ I_c Rh^{III} = 0.54 for **1** and 0.56 for **2**), as shown in Fig. 6. The first reduction peak is metal-centred, for Rh^{III} complexes it is in fact a composite wave corresponding to a two-electron process^{22–25,35} (Rh^{III}→Rh^I). For Rh^{II} complexes it is a one-electron process (Rh^{II}→Rh^I), which is consistent with the observed difference in cathodic current for the first peak. The other two reductions are ligand based. The similarity in the

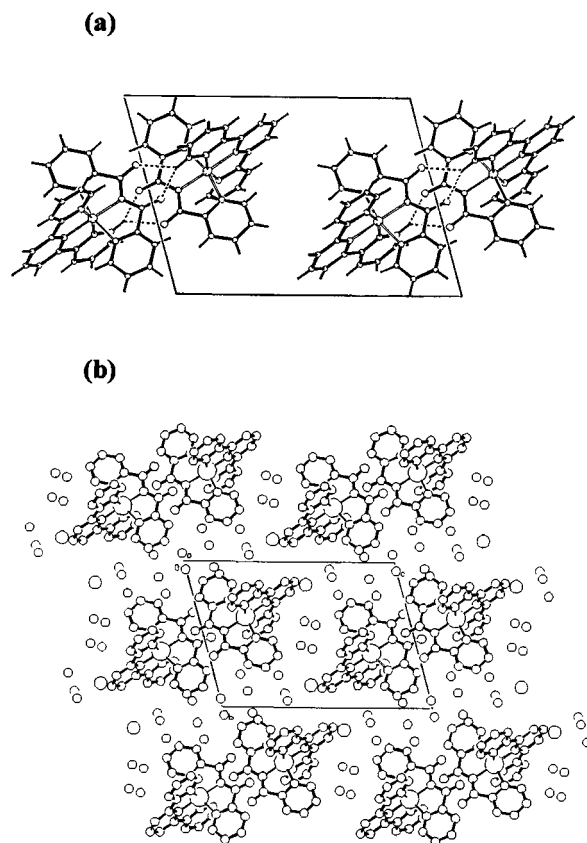


Fig. 4 (a) A view showing the dimeric nature of complex **2** via C-H...O interactions; (b) packing diagram of complex **2** showing the water molecules in the channels around the dimers.

peak potentials of the Rh^{II} and Rh^{III} complexes is probably due to their similar ligand environments. Metal-based two one-electron reduction processes (Rh^{III}→Rh^{II} and Rh^{II}→Rh^I) at the same potential were found by us^{24,25} and others^{10,22,23,35} in many Rh^{III} systems.

EPR spectroscopy

The X-band EPR spectra of complexes **1** and **2** were recorded in acetonitrile at 77 K. The spectrum of **1** is shown in Fig. 7, the g values are $g_{\parallel} = 2.392$ and $g_{\perp} = 2.075$ with hyperfine coupling (doublet) to ¹⁰³Rh ($I = 1/2$) in the g_{\parallel} region ($A_{\parallel} = 155$ G). The g values are reversed from those found in most of the Rh^{II} systems ($g_{\perp} > g_{\parallel}$) but are similar to those found in complexes such as [RhCl₂(PPh₃)₂],^{9,36} [Rh(NO)Cl₃(PPh₃)₂],³⁷ [RhCl₄·2H₂O]²⁻ (studied by X-ray crystallography),³⁸ [RhH₆]⁴⁻ trapped in LiH lattice³⁹ and in a number of Rh^{II} species in zeolite cavities.⁴⁰ The $g_{\parallel} > g_{\perp} \approx g_e$ relationship suggests a $d_{x^2-y^2}$ ground state if the unpaired electron is located on a rhodium(II) ion as a result of a compressed octahedral geometry.^{38–40} The X-ray data for **1** show an axially compressed octahedral geometry of the rhodium which is consistent with

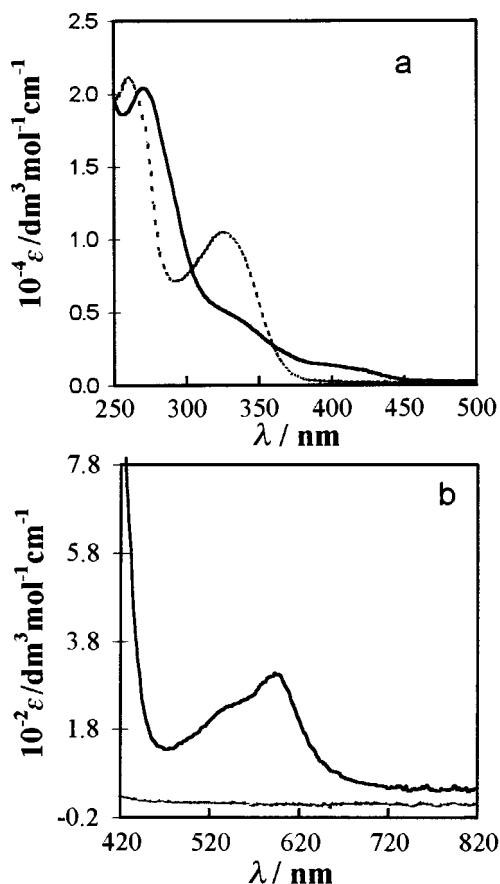


Fig. 5 Electronic absorption spectra of complex **1** (—) and its Rh^{III} analogue, [Rh(bpca)₂][PF₆]₃ (····) in acetonitrile; (a) UV region and (b) visible region.

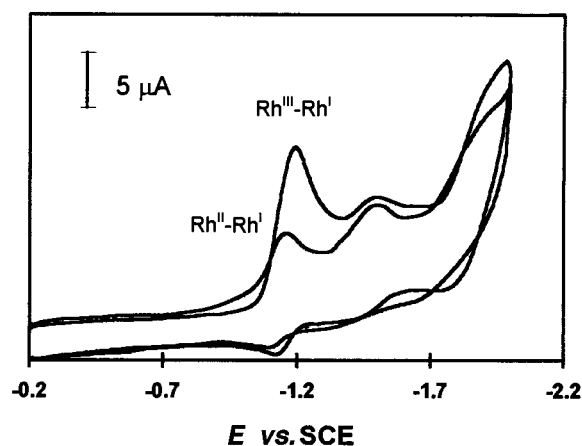


Fig. 6 Cyclic voltammograms of complex **1** and its Rh^{III} analogue, [Rh(bpca)₂][PF₆]₃, recorded in acetonitrile; scan rate 100 mV s⁻¹.

the EPR data. The large A_{\parallel} value (155 G), also found in many other systems, suggests a large amount of spin density at the rhodium nucleus.^{6,41} Complex **2**, however, shows three g values $g_1 = 2.349$, $g_2 = 2.070$ and $g_3 = 1.956$. The g_1 value is close to that of g_{\parallel} of complex **1** and is split into a doublet ($A_1 = 216$ G) due to hyperfine interaction with ¹⁰³Rh. The observed difference in the spectra of **1** and **2** is probably due to the lowering of symmetry which occurs in the mixed ligand complex.

Stability aspects

Six co-ordinate mononuclear rhodium(II) complexes generally possess structural and electronic features that make them susceptible to ligand substitution. Strong interaction of a σ -donor ligand along the z axis destabilises the unpaired electron in the

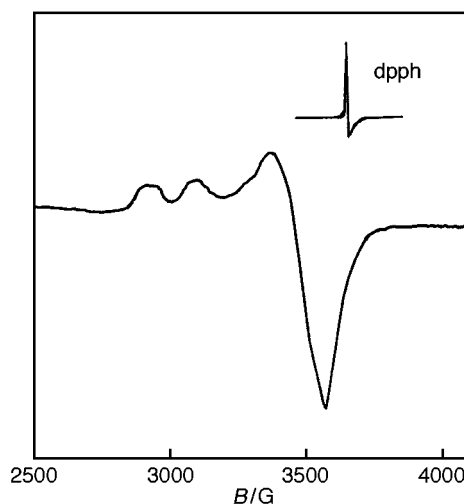


Fig. 7 X-Band EPR spectrum of complex **1** recorded in acetonitrile at 77 K.

d_{z^2} orbital resulting in ligand lability. This effect causes either a disproportionation reaction [Rh(III) and Rh(I)] or dimerisation with the Rh–Rh bond utilising the d_{z^2} orbital.^{6,7} However, it is evident that the steric and electronic effects of the ligands influence the stability of the mononuclear rhodium(II) complexes. Factors which can stabilise the mononuclear rhodium(II) complexes are: bulky ligands which protect the metal ion from external attack, the σ -donor and π -donor–acceptor capabilities of the ligand and the presence of a delocalized π -system in the ligand backbone.⁷ In complexes **1** and **2** the X-ray (axial Rh–N < equatorial Rh–N distances) and EPR data ($g_{\parallel} > g_{\perp}$) suggest a compressed octahedral geometry about the rhodium centre, indicating the unpaired electron to be in the $d_{x^2-y^2}$ orbital. Since the unpaired electron is no longer in the d_{z^2} orbital, ligand lability due to destabilisation of the d_{z^2} orbital did not occur. The strong tridentate chelate effect of the bpca and tpy moieties also protected the periphery of the complex from external attack. The presence of a delocalised π -system (pyridyl ring) in the ligand backbone also contributed to the stabilisation of the rhodium(II). The formation of stable Rh(II) as well as Rh(III) complexes with the same or similar ligands has been reported earlier.^{10,12}

Conclusions

The metal-promoted hydrolysis of tptz afforded a class of complexes containing the ligand bis(2-pyridylcarbonyl)amide anion which provides the necessary structural and electronic requirement to stabilise mononuclear paramagnetic Rh^{II} complexes. To our knowledge these are the first examples of structurally characterised mononuclear Rh^{II} complexes containing poly(pyridyl) ligands. Therefore, it is a significant contribution in the area of mononuclear rhodium(II) chemistry.

Acknowledgements

We are grateful to the Department of Science and Technology (DST), Government of India, for financial support. Our sincere thanks go to Dr S. D. Gomkale, Dr R. V. Jasra and Professor P. Natarajan for their keen interest, encouragement and valuable suggestions in this work. Dr D. Srinivas and Mr Paresh C. Dave are thanked for recording the EPR spectra. We also thank Dr Parthasarathi Dastidar for assistance with the crystallographic study.

References

- 1 T. R. Felthouse, *Prog. Inorg. Chem.*, 1982, **29**, 73.
- 2 E. B. Boyar and S. D. Robinson, *Coord. Chem. Rev.*, 1983, **50**, 109.
- 3 F. P. Pruchnik, *Pure Appl. Chem.*, 1989, **61**, 795.

- 4 L. Natkaniec and F. P. Pruchnik, *J. Chem. Soc., Dalton Trans.*, 1994, 3261.
- 5 F. P. Pruchnik, F. Robert, Y. Jeannin and S. Jeannin, *Inorg. Chem.*, 1996, **35**, 4261.
- 6 K. K. Pandey, *Coord. Chem. Rev.*, 1992, **121**, 1.
- 7 D. G. DeWit, *Coord. Chem. Rev.*, 1996, **147**, 209.
- 8 N. G. Connelly, D. J. H. Emslie, B. Metz, A. G. Orpen and M. J. Quayle, *Chem. Commun.*, 1996, 2289.
- 9 C. A. Ogle, T. C. Masterman and J. L. Hubbard, *J. Chem. Soc., Chem. Commun.*, 1990, 1733.
- 10 S. C. Haefner, K. R. Dunbar and C. Bender, *J. Am. Chem. Soc.*, 1991, **113**, 9540.
- 11 K. R. Dunbar and S. C. Haefner, *Organometallics*, 1992, **11**, 1431.
- 12 R. L. Harlow, D. L. Thorn, R. T. Baker and N. L. Jones, *Inorg. Chem.*, 1992, **31**, 993.
- 13 R. S. Hay-Motherwell, S. U. Koschmieder, G. Wilkinson, B. Hussain-Bates and M. B. Hursthouse, *J. Chem. Soc., Dalton Trans.*, 1991, 2821.
- 14 M. P. Garcia, M. V. Jimenez, L. A. Oro, F. J. Lahoz, J. M. Casas and P. J. Alonso, *Organometallics*, 1993, **12**, 3257.
- 15 S. Peng, *Inorg. Chim. Acta*, 1985, **101**, L35.
- 16 K. R. Dunbar and S. C. Haefner, *Inorg. Chem.*, 1992, **31**, 3676.
- 17 T. Glowiak, H. Pasternak and F. Pruchnik, *Acta Crystallogr., Sect. C*, 1987, **43**, 1036.
- 18 B. Martin, W. R. McWhinnie and G. M. Waind, *J. Inorg. Nucl. Chem.*, 1961, **23**, 207.
- 19 G. M. Brown, S. F. Chan, C. Creutz, H. A. Schwartz and N. Sutin, *J. Am. Chem. Soc.*, 1979, **101**, 7638.
- 20 Q. G. Mulazzani, S. Emmi, M. Z. Hoffman and M. Venturi, *J. Am. Chem. Soc.*, 1981, **103**, 3362.
- 21 H. A. Schwarz and C. Creutz, *Inorg. Chem.*, 1983, **22**, 707.
- 22 G. Kew, K. DeArmond and K. Hanck, *J. Phys. Chem.*, 1974, **78**, 727.
- 23 G. Kew, K. Hanck and K. DeArmond, *J. Phys. Chem.*, 1975, **79**, 1828.
- 24 P. Paul, B. Tyagi, M. M. Bhadbhade and E. Suresh, *J. Chem. Soc., Dalton Trans.*, 1997, 2273.
- 25 P. Paul, B. Tyagi, A. K. Bilakhiya, M. M. Bhadbhade, E. Suresh and G. Ramachandraiah, *Inorg. Chem.*, 1998, **37**, 5733.
- 26 E. I. Gabe, Y. LePage, I. P. Charland, F. L. Lee and P. S. White, *J. Appl. Crystallogr.*, 1989, **22**, 384.
- 27 G. M. Sheldrick, *Acta. Crystallogr., Sect. A*, 1990, **46**, 467.
- 28 G. M. Sheldrick, SHELXL 97, Program for refinement of crystal structures, University of Göttingen, 1997.
- 29 I. Vickovic, Crystal Structure Utility (CSU), a highly automated program for the calculation of geometrical parameters in the crystal structure analysis, Faculty of Science, University of Zagreb, Yugoslavia, 1988.
- 30 B. R. James and D. V. Stynes, *J. Am. Chem. Soc.*, 1972, **94**, 6225.
- 31 C. K. Johnson, ORTEP II, Report ORNL-5138, Oak Ridge National Laboratory, TN, 1976.
- 32 G. R. Desiraju, *Acc. Chem. Res.*, 1991, **24**, 290; *Angew. Chem., Int. Ed. Engl.*, 1995, **34**, 2311.
- 33 S. M. Peng, K. Peters, E. M. Peters and A. Simon, *Inorg. Chim Acta*, 1985, **101**, L35.
- 34 G. P. Kakis and P. Saroulis, *Inorg. Chim. Acta*, 1980, **46**, 97.
- 35 S. C. Rasmussen, M. M. Richter, E. Yi, H. Place and K. J. Brewer, *Inorg. Chem.*, 1990, **29**, 3926.
- 36 J. A. Osborn, F. J. Jardine, J. F. Young and G. Wilkinson, *J. Chem. Soc. A*, 1966, 1711.
- 37 M. C. Baird, *Inorg. Chim Acta*, 1971, **5**, 46.
- 38 M. D. Sastry, K. Savitri and B. D. Joshi, *J. Chem. Phys.*, 1980, **73**, 5568.
- 39 G. C. Abell and R. C. Bowman, Jr., *J. Chem. Phys.*, 1979, **70**, 2611.
- 40 D. Goldfarb and L. Kevan, *J. Phys. Chem.*, 1986, **90**, 264, 2137 and 5787.
- 41 C. Bianchini, P. Frediani, F. Laschi, A. Meli, F. Vizza and P. Zonello, *Inorg. Chem.*, 1990, **29**, 3402.

Paper 9/00757A